Published OnlineFirst October 26, 2010; DOI:10.1158/1078-0432.CCR-10-0581

(Table 3; ref. 31). Partial losses at 3q were also frequently detected (19 of 25; 76%), and a minimal common overlapping region was identified at 3q26.1, although this region contains no annotated genes (Supplementary Table S3). In addition, losses at 4q13.2, the locus of *UGT2B17/UGT2B28*, were detected in 20 of 25 tumors (80%). Losses at 9p were found in 11 of 25 (44%) GISTs, and 4 tumors showed a loss of the whole p-arm. Among seven tumors with partial 9p losses, four showed a loss at 9p21, the locus of *CDKN2A/CDKN2B*.

Losses at 3q, 4q, 14q, and 22q were found to be equally distributed in tumors with all levels of *LINE-1* methylation (Table 3). By contrast, many other chromosomal aberrations correlated with *LINE-1* hypomethylation (Table 3; Fig. 3A). For example, GISTs with losses at 1p showed significantly lower *LINE-1* methylation than those without 1p loss (53.8% versus 64.1%; $P = 0.007$). *LINE-1* methylation was also much lower in tumors with loss at 9p than in those without that loss (52.1% versus 62.5%; $P = 0.005$). Bivariate correlation analysis revealed a significant inverse correlation between levels of *LINE-1* methylation and the total number of chromosomal aberrations, including both losses and gains (Fig. 3B). These results suggest a significant relationship between *LINE-1* hypomethylation and DNA copy number abnormalities in GIST.

Discussion

Although several studies have shown that genetic abnormalities, including various mutations and chromosomal imbalances, are significantly involved in the development of GISTs, little is known about the role played by epigenetic alterations in these tumors. To date, there had been only a few reports of CpG island methylation in GISTs (21–24), and levels of global DNA methylation had not yet been analyzed. In the present study, however, we found that levels of methylation of *LINE-1* and other repetitive elements are reduced in GISTs. It has been known for decades that global hypomethylation is a common feature of human cancer (33, 34), and in recent years, hypomethylation has been studied in various human malignancies using *LINE-1* and other repetitive sequences as surrogates

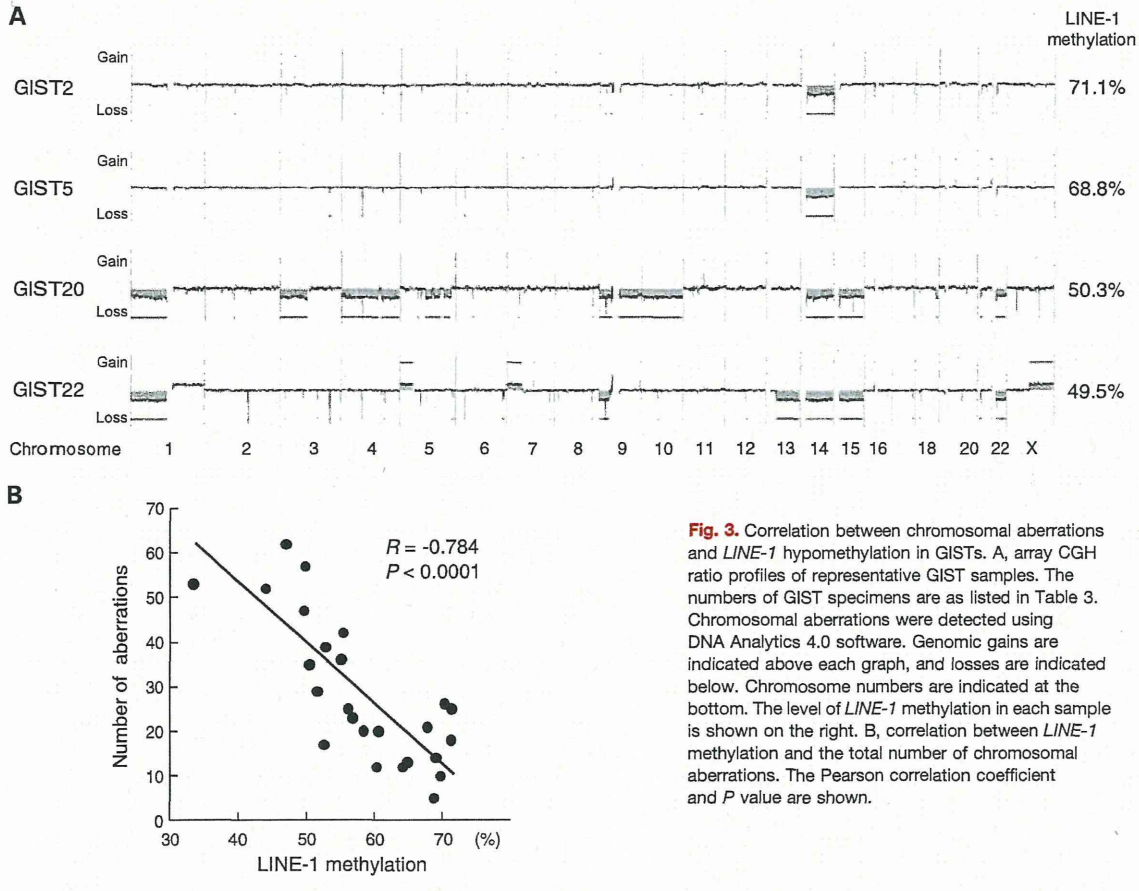

Fig. 3. Correlation between chromosomal aberrations and *LINE-1* hypomethylation in GISTs. A, array CGH ratio profiles of representative GIST samples. The numbers of GIST specimens are as listed in Table 3. Chromosomal aberrations were detected using DNA Analytics 4.0 software. Genomic gains are indicated above each graph, and losses are indicated below. Chromosome numbers are indicated at the bottom. The level of *LINE-1* methylation in each sample is shown on the right. B, correlation between *LINE-1* methylation and the total number of chromosomal aberrations. The Pearson correlation coefficient and *P* value are shown.

Published OnlineFirst October 26, 2010; DOI:10.1158/1078-0432.CCR-10-0581

(9–20). Our results confirm that GISTs exhibit a pattern of hypomethylation that is similar to those exhibited by many other human tumors.

We found that *LINE-1* hypomethylation is strongly associated with the aggressiveness of GISTs. Levels of *LINE-1* methylation were significantly lower in high-risk GISTs than in low- or intermediate-risk tumors. In addition, levels of *LINE-1* methylation inversely correlated with tumor size and mitotic counts. These results are consistent with earlier observations that a reduction in global methylcytosine content is associated with malignant potential in cancer, and that it is especially prevalent in metastatic tumors (34). *LINE-1* hypomethylation is also reportedly associated with poor prognosis in prostate (17), colon (35), and ovarian (36) cancers and in chronic myeloid leukemia (11). In normal cells, DNA methylation plays important roles in X-chromosome inactivation, genomic imprinting, and repression of repetitive elements, such as retrotransposons and endogenous retroviruses. Thus, hypomethylation may associate with tumor malignancy through a variety of mechanisms. For example, global hypomethylation is associated with genomic instability (37–40), which may confer a poor prognosis. Hypomethylation can also lead to activation of proto-oncogenes, endogenous retroviruses, or transposable elements, and such transcriptional dysregulation could affect tumor aggressiveness.

We found strong correlations between the level of LINE-1 methylation and methylation of other repetitive elements. *Sat-α* and *NBL2*, which are tandem DNA repeats, are reportedly hypomethylated in various human cancers (15, 16, 20, 41). We observed that methylation of these elements is also reduced in high-risk GISTs, which suggests that a common mechanism may induce and maintain DNA hypomethylation in tumors. On the other hand, *LINE-1* methylation correlated only moderately with *Alu Yb8* methylation, and hypomethylation of *Alu Yb8* was limited, even in high-risk GISTs. Similar modest correlation between *LINE-1* and Alu methylation was also observed in head and neck squamous cell carcinomas and neuroendocrine tumors (18, 42). This lower correlation may simply reflect a difference in assay sensitivity, although it is possible that there are functional and/or biological differences in the regulation of these two types of repetitive DNA elements.

Although global hypomethylation and regional hypermethylation of 5′ CpG islands are common features of neoplasias, the link between the two remains controversial. Recent studies using methylation of *LINE-1* and/or Alu as a marker revealed that global hypomethylation is correlated with CpG island hypermethylation in prostate cancers (17) and neuroendocrine tumors (42). In addition, we recently showed that *LINE-1* hypomethylation and CpG island hypermethylation are tightly linked in enlarged fold gastritis (14). By contrast, others did not find a similar relationship in Wilm's tumor (41), colon cancer (43), or ovarian cancer (16). Recent studies also revealed that *LINE-1* hypomethylation is inversely correlated with microsatellite instability and/or the CpG island methylator phenotype in colon cancer, suggesting that CpG island hypermethylation and global hypomethylation may reflect different tumor progression pathways (12, 13). In the present study, we failed to find a significant correlation between 5′ CpG island hypermethylation of tumor-related genes and global hypomethylation. However, this may reflect a bias toward selection of genes frequently methylated in tumors of epithelial origin, as GISTs may exhibit methylation of a different spectrum of genes.

House et al. (21) reported that hypermethylation of *CDH1* (*E-cadherin*) is positively correlated with GISTs having malignant histologic features (mitotic rate, tumor size, and necrosis) and a poor prognosis. In addition, the presence of *CDH1* methylation and the absence of *MLH1* methylation correlated with early tumor recurrence. By contrast, Saito et al. (24) reported that CpG island hypermethylation, including that of *MLH1* and *CDH1*, was frequently detected in GISTs, irrespective of their malignancy. In the present study, we found tendencies for *CDH1* methylation to occur more frequently and *MLH1* methylation to occur less frequently in higher-risk GISTs, although these correlations were not statistically significant. We also noticed that the frequencies of CpG island methylation were lower than those reported previously (21, 24). This could reflect differences in the primer sequences used in our study, but the actual reason for the discrepancy is not clear. As mentioned above, GISTs may exhibit hypermethylation of a different spectrum of genes, and further study will be needed to clarify the role of CpG island methylation in GISTs.

Global hypomethylation is strongly implicated in chromosomal instability. A study using $Nf1^{+/-}$ $p53^{+/-}$ mice has shown that introduction of a hypomorphic *Dnmt1* allele causes DNA hypomethylation that leads to significant increases in the loss of heterozygosity rate and tumor development (37). Another study has shown that hypomethylation in $Apc^{Min/+}$ mice leads to increases in microadenoma formation through loss of heterozygosity at the *Apc* locus (38). Global hypomethylation also correlates with chromosomal instability and copy number changes in human cancers (18, 19, 39, 40). Thus, to assess the potential implication of *LINE-1* hypomethylation in genomic instability in GISTs, we carried out an array CGH analysis and correlated hypomethylation with chromosomal imbalances. The results of this analysis are largely consistent with previously reported cytogenetic, CGH, and array CGH analyses of GISTs (28–32). In general, losses were more common than gains, and genomic losses frequently affected 1p, 14q, 15q, and 22q. In addition, we found losses at 3q26.1 and 4q13.2, the locus of *UGT2B17/UGT2B28*, in the majority of tumors tested. UGT2B17, which is a member of the UDP-glucuronosyltransferases (UGT) family, has been implicated in the metabolism of androgens, and a deletion polymorphism in *UGT2B17* is reportedly associated with the risk of prostate cancer (44), although its functional role in GISTs remains to be clarified.

Published OnlineFirst October 26, 2010; DOI:10.1158/1078-0432.CCR-10-0581

Although the most frequent aberrations (e.g., losses of 14q and 22q) were equally distributed among GISTs with all levels of *LINE-1* methylation, we found a significant correlation between many other chromosomal aberrations and DNA hypomethylation. For instance, tumors with losses at 1p or 9p showed significantly lower *LINE-1* methylation. Notably, these results are consistent with previous findings that losses at 14q and 22q are early changes in GIST development, whereas losses at 1p and 9p are associated with malignancy and poor prognosis (28–31). Moreover, total numbers of chromosomal aberrations are highly correlated with *LINE-1* hypomethylation. It thus seems that *LINE-1* hypomethylation may play an important role in inducing chromosomal aberrations and increasing the aggressiveness of GISTs. Currently, however, we have no functional evidence of a causal relationship between hypomethylation and the genomic instability of GISTs, and further studies will be required to clarify the underlying molecular mechanism.

In summary, we found that hypomethylation of repetitive elements is associated with high-risk GISTs. We also provide further evidence that *LINE-1* hypomethylation is strongly associated with chromosomal aberrations. Although the cause of DNA hypomethylation in GISTs remains unclear, *LINE-1* methylation could be a useful marker for predicting the risk and prognosis of the disease.

Disclosure of Potential Conflicts of Interest

No potential conflicts of interest were disclosed.

Acknowledgments

We thank Dr. William F. Goldman for editing the manuscript and M. Ashida for technical assistance.

Grant Support

Grants-in-Aid for Scientific Research on Priority Areas (M. Toyota and K. Imai), Program for developing the supporting system for upgrading the education and research from the Ministry of Education, Culture, Sports, Science, and Technology (Y. Shinomura and M. Toyota), A3 foresight program from the Japan Society for Promotion of Science (H. Suzuki), Grants-in-Aid for Scientific Research (B) from the Japan Society for Promotion of Science (Y. Shinomura), Grants-in-Aid for Scientific Research (S) from the Japan Society for Promotion of Science (K. Imai), a Grant-in-Aid for the Third-term Comprehensive 10-year Strategy for Cancer Control (M. Toyota), and a Grant-in-Aid for Cancer Research from the Ministry of Health, Labor, and Welfare, Japan (M. Toyota).

The costs of publication of this article were defrayed in part by the payment of page charges. This article must therefore be hereby marked *advertisement* in accordance with 18 U.S.C. Section 1734 solely to indicate this fact.

Received 03/06/2010; revised 06/08/2010; accepted 06/20/2010; published OnlineFirst 10/26/2010.

References

1. Shinomura Y, Kinoshita K, Tsutsui S, et al. Pathophysiology, diagnosis, and treatment of gastrointestinal stromal tumors. J Gastroenterol 2005;40:775–80.
2. Rubin BP, Heinrich MC, Corless CL. Gastrointestinal stromal tumour. Lancet 2007;369:1731–41.
3. Yang J, Du X, Lazar AJ, et al. Genetic aberrations of gastrointestinal stromal tumors. Cancer 2008;113:1532–43.
4. Fletcher CD, Berman JJ, Corless C, et al. Diagnosis of gastrointestinal stromal tumors: a consensus approach. Hum Pathol 2002;33:459–65.
5. Jones PA, Baylin SB. The fundamental role of epigenetic events in cancer. Nat Rev Genet 2002;3:415–28.
6. Suzuki H, Tokino T, Shinomura Y, Imai K, Toyota M. DNA methylation and cancer pathways in gastrointestinal tumors. Pharmacogenomics 2008;9:1917–28.
7. Cordaux R, Batzer MA. The impact of retrotransposons on human genome evolution. Nat Rev Genet 2009;10:691–703.
8. Yang AS, Estécio MR, Doshi K, Kondo Y, Tajara EH, Issa JP. A simple method for estimating global DNA methylation using bisulfite PCR of repetitive DNA elements. Nucleic Acids Res 2004;32:e38.
9. Takai D, Yagi Y, Habib N, Sugimura T, Ushijima T. Hypomethylation of LINE1 retrotransposon in human hepatocellular carcinomas, but not in surrounding liver cirrhosis. Jpn J Clin Oncol 2000;30:306–9.
10. Chalitchagorn K, Shuangshoti S, Hourpai N, et al. Distinctive pattern of LINE-1 methylation level in normal tissues and the association with carcinogenesis. Oncogene 2004;23:8841–6.
11. Roman-Gomez J, Jimenez-Velasco A, Agirre X, et al. Promoter hypomethylation of the LINE-1 retrotransposable elements activates sense/antisense transcription and marks the progression of chronic myeloid leukemia. Oncogene 2005;24:7213–23.
12. Estécio MR, Gharibyan V, Shen L, et al. LINE-1 hypomethylation in cancer is highly variable and inversely correlated with microsatellite instability. PLoS One 2007;2:e399.
13. Ogino S, Kawasaki T, Nosho K, et al. LINE-1 hypomethylation is inversely associated with microsatellite instability and CpG island methylator phenotype in colorectal cancer. Int J Cancer 2008;122:2767–73.
14. Yamamoto E, Toyota M, Suzuki H, et al. LINE-1 hypomethylation is associated with increased CpG island methylation in *Helicobacter pylori*-related enlarged-fold gastritis. Cancer Epidemiol Biomarkers Prev 2008;17:2555–64.
15. Itano O, Ueda M, Kikuchi K, et al. Correlation of postoperative recurrence in hepatocellular carcinoma with demethylation of repetitive sequences. Oncogene 2002;21:789–97.
16. Ehrlich M, Woods CB, Yu MC, et al. Quantitative analysis of associations between DNA hypermethylation, hypomethylation, and DNMT RNA levels in ovarian tumors. Oncogene 2006;25:2636–45.
17. Cho NY, Kim BH, Choi M, et al. Hypermethylation of CpG island loci and hypomethylation of LINE-1 and Alu repeats in prostate adenocarcinoma and their relationship to clinicopathological features. J Pathol 2007;211:269–77.
18. Richards KL, Zhang B, Baggerly KA, et al. Genome-wide hypomethylation in head and neck cancer is more pronounced in HPV-negative tumors and is associated with genomic instability. PLoS One 2009;4:e4941.
19. Daskalos A, Nikolaidis G, Xinarianos G, et al. Hypomethylation of retrotransposable elements correlates with genomic instability in non-small cell lung cancer. Int J Cancer 2009;124:81–7.
20. Choi SH, Worswick S, Byun HM, et al. Changes in DNA methylation of tandem DNA repeats are different from interspersed repeats in cancer. Int J Cancer 2009;125:723–9.
21. House MG, Guo M, Efron DT, et al. Tumor suppressor gene hypermethylation as a predictor of gastric stromal tumor behavior. J Gastrointest Surg 2003;7:1004–14.
22. Ricci R, Arena V, Castri F, et al. Role of p16/INK4a in gastrointestinal stromal tumor progression. Am J Clin Pathol 2004;122:35–43.
23. Perrone F, Tamborini E, Dagrada GP, et al. 9p21 locus analysis in high-risk gastrointestinal stromal tumors characterized for c-kit and platelet-derived growth factor receptor α gene alterations. Cancer 2005;104:159–69.
24. Saito K, Sakurai S, Sano T, et al. Aberrant methylation status of

Published OnlineFirst October 26, 2010; DOI:10.1158/1078-0432.CCR-10-0581

known methylation-sensitive CpG islands in gastrointestinal stromal tumors without any correlation to the state of c-kit and PDGFRA gene mutations and their malignancy. Cancer Sci 2008;99:253–9.
25. Weisenberger DJ, Campan M, Long TI, et al. Analysis of repetitive element DNA methylation by MethyLight. Nucleic Acids Res 2005; 33:6823–36.
26. Weisenberger DJ, Siegmund KD, Campan M, et al. CpG island methylator phenotype underlies sporadic microsatellite instability and is tightly associated with BRAF mutation in colorectal cancer. Nat Genet 2006;38:787–93.
27. Nosho K, Yamamoto H, Takahashi T, et al. Genetic and epigenetic profiling in early colorectal tumors and prediction of invasive potential in pT1 (early invasive) colorectal cancers. Carcinogenesis 2007; 28:1364–70.
28. Kim NG, Kim JJ, Ahn JY, et al. Putative chromosomal deletions on 9P, 9Q and 22Q occur preferentially in malignant gastrointestinal stromal tumors. Int J Cancer 2000;85:633–8.
29. El-Rifai W, Sarlomo-Rikala M, Andersson LC, et al. DNA sequence copy number changes in gastrointestinal stromal tumors: tumor progression and prognostic significance. Cancer Res 2000;60: 3899–903.
30. Gunawan B, Bergmann F, Höer J, et al. Biological and clinical significance of cytogenetic abnormalities in low-risk and high-risk gastrointestinal stromal tumors. Hum Pathol 2002;33:316–21.
31. Wozniak A, Sciot R, Guillou L, et al. Array CGH analysis in primary gastrointestinal stromal tumors: cytogenetic profile correlates with anatomic site and tumor aggressiveness, irrespective of mutational status. Genes Chromosomes Cancer 2007;46:261–76.
32. Assämäki R, Sarlomo-Rikala M, Lopez-Guerrero JA, et al. Array comparative genomic hybridization analysis of chromosomal imbalances and their target genes in gastrointestinal stromal tumors. Genes Chromosomes Cancer 2007;46:564–76.
33. Feinberg AP, Vogelstein B. Hypomethylation distinguishes genes of some human cancers from their normal counterparts. Nature 1983; 301:89–92.
34. Gama-Sosa MA, Slagel VA, Trewyn RW, et al. The 5-methylcytosine content of DNA from human tumors. Nucleic Acids Res 1983;11: 6883–94.
35. Ogino S, Nosho K, Kirkner GJ, et al. A cohort study of tumoral LINE-1 hypomethylation and prognosis in colon cancer. J Natl Cancer Inst 2008;100:1734–8.
36. Pattamadilok J, Huapai N, Rattanatanyong P, et al. LINE-1 hypomethylation level as a potential prognostic factor for epithelial ovarian cancer. Int J Gynecol Cancer 2008;18:711–7.
37. Eden A, Gaudet F, Waghmare A, Jaenisch R. Chromosomal instability and tumors promoted by DNA hypomethylation. Science 2003;300:455.
38. Yamada Y, Jackson-Grusby L, Linhart H, et al. Opposing effects of DNA hypomethylation on intestinal and liver carcinogenesis. Proc Natl Acad Sci U S A 2005;102:13580–5.
39. Karpf AR, Matsui S. Genetic disruption of cytosine DNA methyltransferase enzymes induces chromosomal instability in human cancer cells. Cancer Res 2005;65:8635–9.
40. Rodriguez J, Frigola J, Vendrell E, et al. Chromosomal instability correlates with genome-wide DNA demethylation in human primary colorectal cancers. Cancer Res 2006;66:8462–8.
41. Ehrlich M, Jiang G, Fiala E, et al. Hypomethylation and hypermethylation of DNA in Wilms tumors. Oncogene 2002;21: 6694–702.
42. Choi IS, Estecio MR, Nagano Y, et al. Hypomethylation of LINE-1 and Alu in well-differentiated neuroendocrine tumors (pancreatic endocrine tumors and carcinoid tumors). Mod Pathol 2007;20: 802–10.
43. Iacopetta B, Grieu F, Phillips M, et al. Methylation levels of LINE-1 repeats and CpG island loci are inversely related in normal colonic mucosa. Cancer Sci 2007;98:1454–60.
44. Park J, Chen L, Ratnashinge L, et al. Deletion polymorphism of UDP-glucuronosyltransferase 2B17 and risk of prostate cancer in African American and Caucasian men. Cancer Epidemiol Biomarkers Prev 2006;15:1473–8.

Cell

Premature Termination of Reprogramming In Vivo Leads to Cancer Development through Altered Epigenetic Regulation

Kotaro Ohnishi,[1,2,8] Katsunori Semi,[1,3,8] Takuya Yamamoto,[1,3] Masahito Shimizu,[2] Akito Tanaka,[1] Kanae Mitsunaga,[1] Keisuke Okita,[1] Kenji Osafune,[1] Yuko Arioka,[1] Toshiyuki Maeda,[4] Hidenobu Soejima,[4] Hisataka Moriwaki,[2] Shinya Yamanaka,[1,3,5] Knut Woltjen,[1,6] and Yasuhiro Yamada[1,3,7,*]

[1]Center for iPS Cell Research and Application (CiRA), Kyoto University, Kyoto 606-8507, Japan
[2]Department of Medicine, Gifu University Graduate School of Medicine, Gifu 501-1194, Japan
[3]Institute for Integrated Cell-Material Sciences (WPI-iCeMS), Kyoto University, Kyoto 606-8507, Japan
[4]Division of Molecular Genetics and Epigenetics, Department of Biomolecular Sciences, Faculty of Medicine, Saga University, Saga 849-8501, Japan
[5]Gladstone Institute of Cardiovascular Disease, San Francisco, CA 94158, USA
[6]Hakubi Center for Advanced Research, Kyoto University, Kyoto 606-8507, Japan
[7]PRESTO, Japan Science and Technology Agency, 4-1-8 Honcho Kawaguchi, Saitama, 332-0012, Japan
[8]These authors contributed equally to this work
*Correspondence: y-yamada@cira.kyoto-u.ac.jp
http://dx.doi.org/10.1016/j.cell.2014.01.005

SUMMARY

Cancer is believed to arise primarily through accumulation of genetic mutations. Although induced pluripotent stem cell (iPSC) generation does not require changes in genomic sequence, iPSCs acquire unlimited growth potential, a characteristic shared with cancer cells. Here, we describe a murine system in which reprogramming factor expression in vivo can be controlled temporally with doxycycline (Dox). Notably, transient expression of reprogramming factors in vivo results in tumor development in various tissues consisting of undifferentiated dysplastic cells exhibiting global changes in DNA methylation patterns. The Dox-withdrawn tumors arising in the kidney share a number of characteristics with Wilms tumor, a common pediatric kidney cancer. We also demonstrate that iPSCs derived from Dox-withdrawn kidney tumor cells give rise to nonneoplastic kidney cells in mice, proving that they have not undergone irreversible genetic transformation. These findings suggest that epigenetic regulation associated with iPSC derivation may drive development of particular types of cancer.

INTRODUCTION

Induced pluripotent stem cells (iPSCs) can be established from differentiated somatic cells by the forced induction of four transcription factors: *Oct3/4*, *Klf4*, *Sox2*, and *c-Myc* (Takahashi et al., 2007; Takahashi and Yamanaka, 2006; Maherali et al., 2007; Okita et al., 2007; Wernig et al., 2007; Woltjen et al., 2009). To achieve somatic cell reprogramming, multiple cellular processes act synergistically in a sequential manner (Brambrink et al., 2008; Polo et al., 2012; Samavarchi-Tehrani et al., 2010). Despite extensive studies, the precise mechanism of somatic cell reprogramming still remains unclear (Rais et al., 2013). It is known that non-iPSC-like colonies often appear at the intermediate stage of cellular reprogramming in vitro. In addition, there are several reports describing partial iPSCs that deviate successful reprogramming (Fussner et al., 2011; Mikkelsen et al., 2008; Sridharan et al., 2009). However, the characteristics of such failed reprogramming states are largely unknown, and no study has elucidated the failed reprogramming state from cell types other than fibroblasts.

The process of iPSC derivation shares many characteristics with cancer development. During reprogramming, somatic differentiated cells acquire the properties of self-renewal along with unlimited proliferation and exhibit global alterations of the transcriptional program, which are also critical events during carcinogenesis (Ben-Porath et al., 2008). The metabolic switch to glycolysis that occurs during somatic cell reprogramming is similarly observed in cancer development (Folmes et al., 2011). Such similarities suggest that reprogramming processes and cancer development may be partly promoted by overlapping mechanisms (Hong et al., 2009). Practically, the forced induction of the critical reprogramming factor *Oct3/4* in adult somatic cells results in dysplastic growth in epithelial tissues through the inhibition of cellular differentiation in a manner similar to that in embryonic cells (Hochedlinger et al., 2005). These studies provided a possible link between transcription-factor-mediated reprogramming and cancer development.

To elucidate the involvement of failed reprogramming in cancer development, in the present study, we generated an in vivo reprogramming mouse system using reprogramming factor-inducible alleles and examined the effects of reprogramming factor expression in somatic cells in vivo. We show that failed reprogramming-associated cells behave similarly to cancer cells

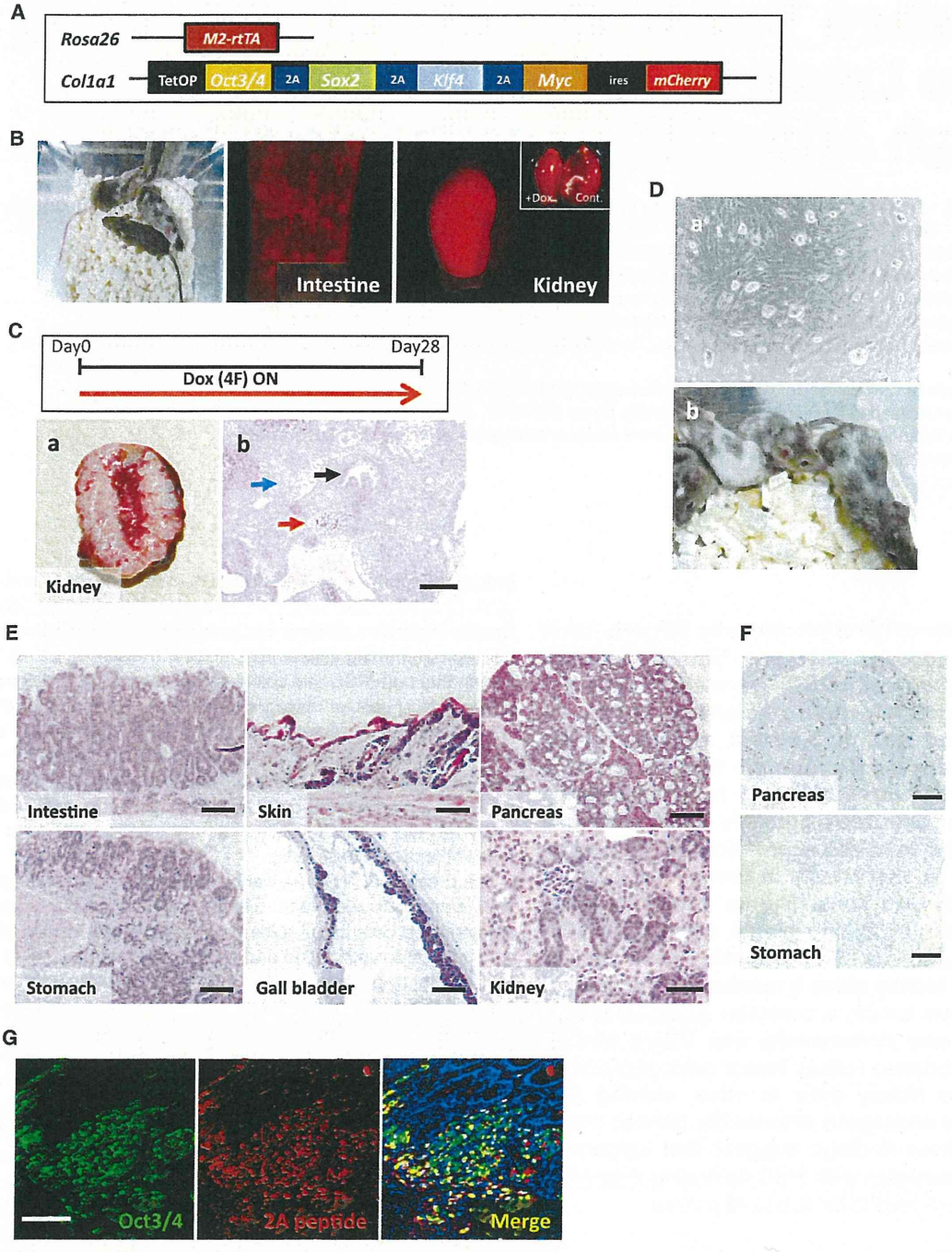

Figure 1. Reprogramming of Somatic Cells In Vivo

(A) Generation of four-factor-inducible ESCs. TetOP, tetracycline-dependent promoter.

(B) Generation of chimeric mice using OSKM-inducible ESCs. mCherry signals could be detected in various organs after Dox treatment for 3 days.

(C) Treatment of chimeric mice with Dox for 28 days resulted in the development of multiple tumors containing pluripotent stem cells. (a) A representative macroscopic image of the cut surface of the kidney tumor. (b) A histological section of the kidney tumor showing the differentiation of tumor cells into three germ layers, indicating teratoma formation. The blue, red, and black arrows represent neuronal, cartilage, and glandular epithelial components, respectively. Scale bar, 200 μm.

(legend continued on next page)

and cause neoplasia resembling Wilms tumor, a childhood blastoma in the kidney. Moreover, we demonstrate that altered epigenetic regulations cause the abnormal growth of such failed reprogramming-associated cancer cells.

RESULTS

In Vivo Reprogrammable Mouse

To establish the reprogrammable mouse system, we generated embryonic stem cells (ESCs) in which reprogramming factors can be induced under the control of doxycycline (Dox) (Figure 1A) (Carey et al., 2010; Stadtfeld et al., 2010b). We used KH2 ESCs with the optimized reverse tetracycline-dependent transactivator at the *ROSA 26* locus (Beard et al., 2006). A polycistronic cassette encoding four reprogramming factors (*Oct3/4*, *Sox2*, *Klf4*, and c-*Myc*) (Carey et al., 2010), followed by *ires-mCherry*, was targeted into the *Col1a1* gene locus under the tetracycline-dependent promoter of KH2 ESCs (Figure 1A).

Next, we generated chimeric mice via blastocyst injection of four-factor (4F)-inducible ESCs. To confirm inducible expression of the reprogramming factors and mCherry in vivo, Dox-containing water was provided to chimeric mice starting at 4 weeks of age. On day 3 of Dox treatment, we could detect the mCherry signal in various organs, including stomach, intestine, liver, pancreas, kidney, gallbladder, and skin (Figure 1B). We also confirmed the expression of reprogramming factors in germline-transmitted mouse tissues by quantitative RT-PCR (qRT-PCR) (Figure S1A available online).

Mouse embryonic fibroblasts (MEFs) containing these reprogramming factor-inducible alleles could give rise to iPSCs after Dox treatment in vitro (Figure S1B). We next asked whether responding somatic cells could be reprogrammed in vivo. The chimeric and germline-transmitted mice given Dox-containing water (2 mg/ml) from 4 weeks of age became morbid within 7–10 days and a few days, respectively. A small proportion of chimeric mice could be treated with Dox for 4 weeks, presumably because of a lower contribution of ESCs in responding tissues. Notably, mice treated with Dox for 4 weeks developed multiple tumors in several organs, such as the kidney and pancreas (Figure 1Ca), whereas tumor formation was never observed in nontreated mice (n = 7, 7 months of age). Histological analysis revealed that these tumors differentiated into three different germ layers, indicating that they are teratomas (Figure 1Cb). When teratoma cells were cultured ex vivo in the absence of Dox (no additional 4F expressions), iPSC-like cells were established (Figure 1Da). Importantly, the teratoma-derived iPSC-like cells contributed to adult chimeric mice when they were injected into blastocysts (Figure 1Db). Therefore, we conclude that somatic cells can be reprogrammed in vivo to pluripotency in our reprogrammable mouse system.

Forced Expression of Reprogramming Factors In Vivo Leads to Rapid Expansion of Dysplastic Cells

We next examined the early changes after expression of reprogramming factors in somatic cells in vivo. After treatment of 4-week-old mice with Dox for 3–9 days, all mice developed dysplastic lesions in epithelial tissues of various organs (Figure 1E), although there were variations in severity of the phenotype among chimeras. Dysplastic cells proliferated actively, as revealed by Ki67 staining (Figure 1F). Abnormal proliferation of somatic cells was observed as early as 3 days after Dox treatment (Figure S1C), and by day 7, such dysplastic cell growth was detected even for pancreatic and kidney cells, which typically do not divide actively under physiological conditions (Figures 1E and 1F). Immunofluorescent analysis of Oct3/4 and the 2A peptide (forming transgene connections) demonstrated that the dysplastic cells expressed reprogramming factors (Figure 1G). Collectively, the forced expression of reprogramming factors caused dysplastic cell expansion of epithelial tissues in vivo.

The Fate of Early Dysplastic Cells after Withdrawal of Dox

To examine whether subsequent expansion of such dysplastic cells depends on the continuous expression of reprogramming factors, we withdrew Dox for 7 days after an initial 4- to 7-day treatment (Figure 2A). Although Dox treatment for 4–7 days caused active cell proliferation in a variety of tissues of all mice, we did not observe any dysplastic cells in some mice after withdrawal of Dox (Figure 2A; Table 1). Of particular note, mice treated with Dox for periods less than 5 days before withdrawal often revealed a lack of dysplastic cells (Table 1). These data suggest that early dysplastic cell growth requires continuous expression of reprogramming factors. We next investigated the fate of eliminated dysplastic proliferating cells after the withdrawal of Dox. Bromodeoxyuridine (BrdU) was injected into mice during Dox treatment to label proliferating cells caused by reprogramming factor expression during the first 7 days (Hochedlinger et al., 2005), and then mice were sacrificed after the withdrawal of Dox for 7 days, on day14. Notably, BrdU-labeled cells were often observed in normal-looking pancreatic and kidney tissues at day14 (Figure 2B). Furthermore, BrdU-labeled cells in the pancreatic islets also expressed insulin (Figure 2B). This suggests that the expanded cells caused by the transient expression of reprogramming factors were, at least in part, integrated into normal-looking tissues after Dox withdrawal.

(D) Teratomas contain pluripotent stem cells. (a) Ex vivo teratoma culture gave rise to iPSC-like colonies without Dox exposure. (b) Teratoma-derived iPSCs contributed to adult chimeric mice.

(E) Dysplastic cell expansion by the forced expression of reprogramming factors in vivo. The histology of various organs of mice treated with Dox for 3 to 9 days. Scale bars, 200 μm (intestine, skin, pancreas, stomach, and gall bladder) and 100 μm (kidney).

(F) Ki67 immunostaining revealed active proliferation of the dysplastic cells in the pancreas and stomach. Scale bars, 200 μm.

(G) Immunofluorescent staining for Oct3/4 and 2A peptide in the intestine of an OSKM chimeric mouse treated with Dox for 7 days. The 2A antibody used here recognizes both Oct3/4-P2A and Sox2-T2A. Dysplastic cells showed positive staining for both Oct3/4 and 2A. Scale bar, 50 μm.

See also Figure S1.

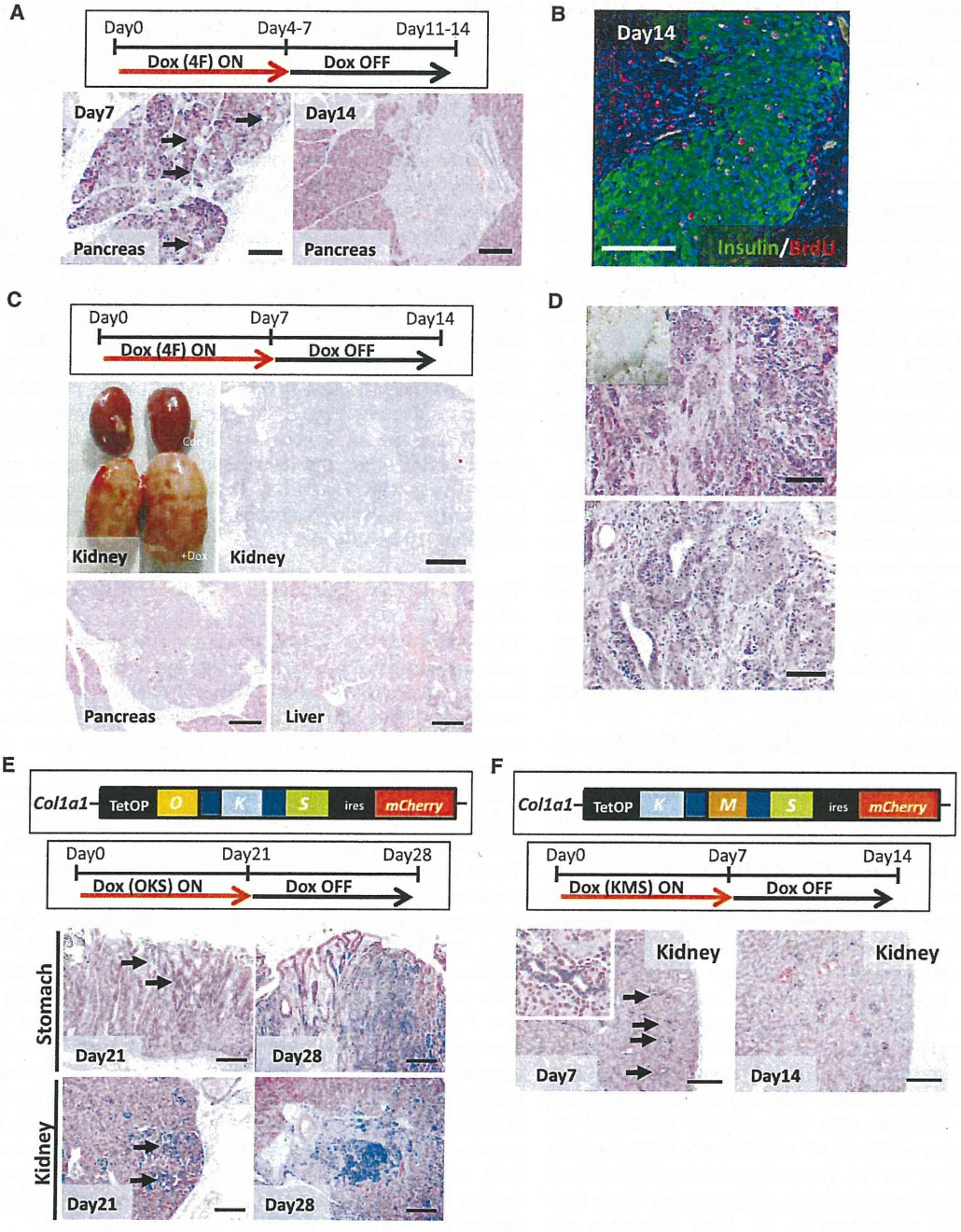

Figure 2. Transient Expression of Reprogramming Factors Causes Neoplasia

(A) A schematic drawing of the experiment and histological sections of the pancreas taken on days 7 and 14. Dysplastic cell growth was induced by treatment with Dox for 7 days (arrows on day 7). The pancreatic section taken on day 14 revealed normal histology. Scale bars, 200 μm.

(B) Double immunofluorescence for insulin and BrdU in the pancreas on day 14. For the pulse and chase experiment, BrdU was injected intraperitoneally every day during Dox administration starting on day 2 (days 2–7), followed by withdrawal of Dox for 7 days. BrdU-positive cells were frequently observed in normal-looking pancreatic islet cells, which also expressed insulin. Scale bar, 100 μm.

(C) Treatment of OSKM chimeric mice with Dox for 7 days, followed by the withdrawal of Dox for another 7 days. The macroscopic image shows the development of bilateral kidney tumors on day 14. Representative histological images are shown for Dox-withdrawn tumors in the kidney, pancreas, and liver. Scale bars, 200 μm.

(legend continued on next page)

Table1. Transient Expression of Reprogramming Factors Causes Tumor Development

		Kidney		Pancreas		Liver	
Dox Treatment	n	No Phenotype	Dysplastic Growth	No Phenotype	Dysplastic Growth	No Phenotype	Dysplastic Growth
4 days ON→OFF	4	2	2	4	0	3	1
5 days ON→OFF	2	1	1	2	0	2	0
6 days ON→OFF	5	1	4	2	3	3	2
7 days ON→OFF	33	7	26	22	11	25	8

Prolonged Expression of Reprogramming Factors Leads to Transgene-Independent Tumor Formation in Somatic Cells

In contrast to the reversion of early dysplastic proliferating cells into normal-looking cells, mice that had been given Dox for 7 days often went on to develop tumors in multiple responding organs even after Dox withdrawal (Figure 2C; Table 1). The developed tumors consisted of histologically undifferentiated dysplastic cells, which were distinct from teratoma cells (Figures 2C and S2A). The dysplastic cells invaded the surrounding tissues, which is one of the hallmarks of cancer cell growth (Figure S2A). Dox-withdrawn tumor cells were negative for 2A staining, affirming that they grew independent of transgene expression (Figure S2B). Dox-withdrawn kidney tumors were similarly observed in elderly mice given Dox starting at 14 weeks of age (13 out of 19 mice). When Dox-withdrawn kidney tumor cells were transplanted into the subcutaneous tissues of immunocompromised mice, they formed secondary tumors within 3 weeks without Dox administration (Figures 2D and S2C), reflecting the neoplastic potential of Dox-withdrawn tumor cells.

Reprogramming factors in our transgenic system include *c-Myc*, a well-known oncogene. To investigate the contribution of *c-Myc* on the development of Dox-withdrawn tumors, we generated three-factor-inducible chimeric mice, which express *Oct3/4*, *Sox2*, and *Klf4* (OKS), but not *c-Myc*, by the targeted insertion of transgenes into the identical locus as 4F (OSKM)-inducible mice (Figure 2E). Similar to 4F-induced mice, OKS induction in vivo caused dysplastic cell growth in various organs yet required longer periods of treatment (Figure 2E). After 3 weeks of induction of OKS followed by withdrawal for 7 days, these mice developed the Dox-withdrawn tumors consisting of undifferentiated dysplastic cells in multiple organs (4 out of 8 mice; Figure 2E). Therefore, transgenic *c-Myc* is dispensable for the development of Dox-withdrawn tumors.

Oct3/4 plays a critical role in cellular reprogramming, and expression of three factors (*Klf4*, *c-Myc*, and *Sox2*) in the absence of *Oct3/4* is not sufficient for iPSC generation (Takahashi and Yamanaka, 2006). To further demonstrate a link between cellular reprogramming and Dox-withdrawn tumor development, we generated chimeric mice in which *Klf4*, *c-Myc*, and *Sox2* (KMS), but not *Oct3/4*, can be induced upon Dox treatment (Figure 2F). Following Dox treatment for 7 days, we observed dysplastic cell growth in the kidney of KMS-inducible mice (three out of six mice; Figure 2F). However, in sharp contrast to OSKM/OKS-induced mice, the withdrawal of Dox eliminated the dysplastic cells in the kidney of KMS-induced mice (n = 17; Figure 2F). A previous study demonstrated that ectopic expression of *Oct3/4* alone can induce dysplastic growth whereas the transgene withdrawal leads to complete reversion of such dysplasia (Hochedlinger et al., 2005). Consistent with the previous observation, the *Oct3/4*-single induction under the same experimental condition failed to form Dox-withdrawn tumors (n = 18; Figure S2D). Taken together, we conclude that reprogramming pressure toward pluripotency driven by the combination of reprogramming factors is associated with the development of Dox-withdrawn tumors.

Loss of Cell Identity and Gain of ESC-Related Gene Expression in Dox-Withdrawn Tumors

To characterize Dox-withdrawn tumor cells, we examined gene expression in kidney tumors that arose in OSKM-inducible mice treated with the 7+/7− Dox regimen. In the KH2 system, transgene expression in the kidney is induced exclusively in the tubule cells (Beard et al., 2006). We observed decreased expression of kidney tubule cell-specific genes in Dox-withdrawn kidney tumors, indicating loss of kidney cell identity (Figure 3A). A previous study dissected the gene expression signature of ESCs into three functional modules: core pluripotency factors, Polycomb complex factors, and Myc-related factors (Kim et al., 2010). Notably, microarray analysis revealed that the ESC-Core module is similarly activated in Dox-withdrawn kidney tumors and ESCs (Figure 3B) (Ohta et al., 2013). We also found that the Myc module displays similar activation between Dox-withdrawn tumors and ESCs (Figure S3A). The activation of ESC-Core and ESC-Myc modules was similarly confirmed in transplanted secondary tumors (Figure S3B).

(D) Minced Dox-withdrawn tumor cells were injected in the subcutaneous tissues of immunocompromised mice. A histological section of one of the tumors phenocopied the original Dox-withdrawn tumor. Scale bars, 200 μm (upper panel) and 100 μm (lower panel).

(E) A schematic drawing of the OKS transgene at the *Col1a1* locus. A histological section of the kidney on days 21 and 28. The expansion of dysplastic cells was observed in the stomach and kidneys on day 21 (arrows). The dysplastic cell growth could be detected even after the withdrawal of Dox in OKS-induced mice (day 28). Scale bars, 200 μm.

(F) A schematic drawing of the KMS transgene. A histological section of a kidney after the treatment with Dox for 7 days (day 7) and the withdrawal of Dox for another 7 days (day 14). KMS induction leads to dysplastic growth in the kidney tubule cells (arrows for day 7). The inset shows a higher-magnification image. No dysplastic cells were detectable in the kidneys of KMS-induced mice after the withdrawal of Dox (day 14). Scale bars, 200 μm.

See also Figure S2.

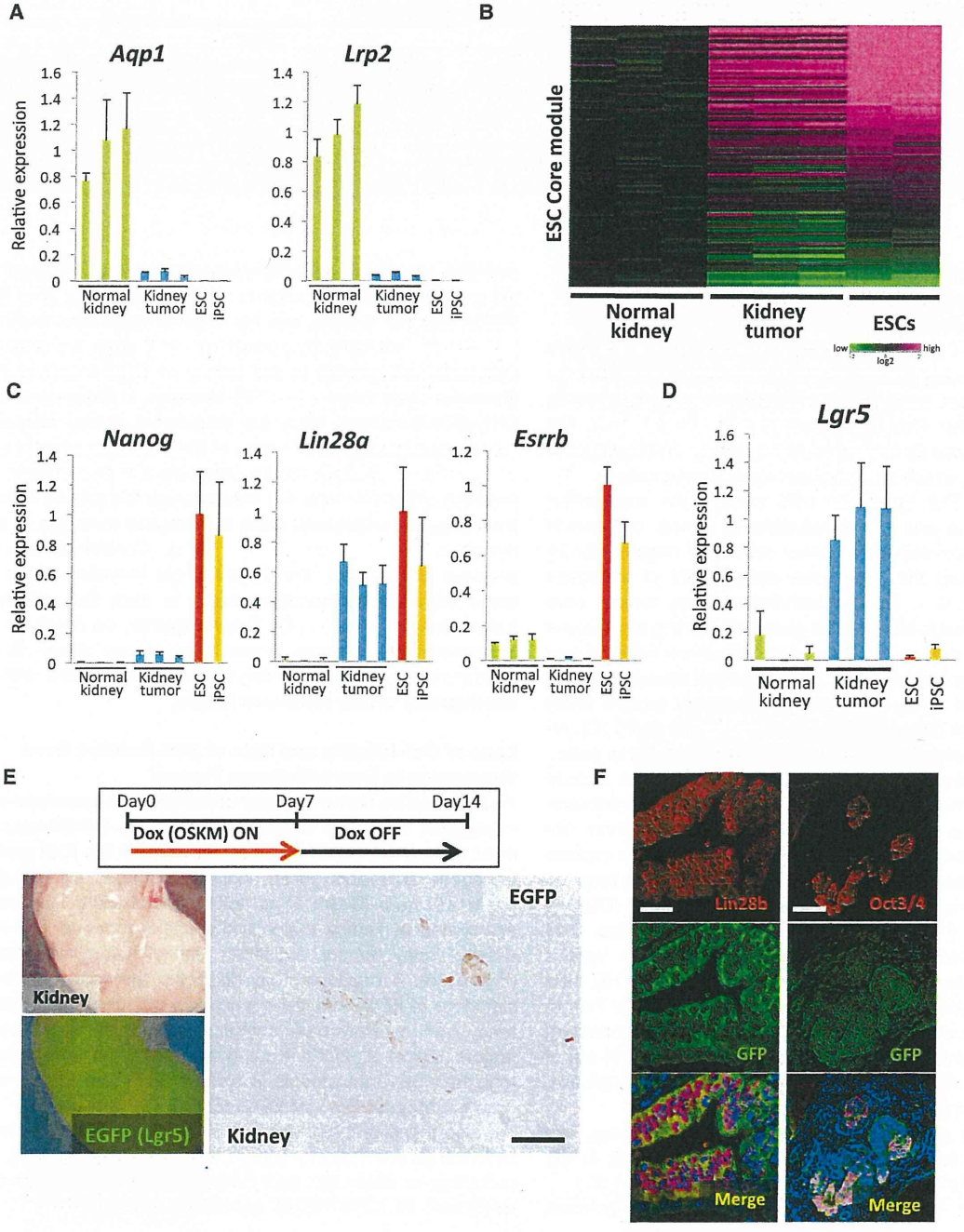

Figure 3. Loss of Cell Identity and Gain of ESC-Related Gene Expression in the Dox-Withdrawn Tumors

(A) The results of the qRT-PCR analyses of *Aqp1* and *Lrp2*. The expression levels of *Aqp1* and *Lrp2* were significantly downregulated in the Dox-withdrawn kidney tumors. Data are presented as mean ± SD. The mean level of normal kidney samples was set to 1.

(B) The microarray analyses revealed the activation of the ESC Core module in Dox-withdrawn kidney tumors.

(C) The results of the qRT-PCR analyses of pluripotency-related genes. Data are presented as mean ± SD. The transcript level in ESCs was set to 1.

(D) *Lgr5* as a candidate marker of Dox-withdrawn kidney tumor cells. *Lgr5* was specifically expressed in Dox-withdrawn kidney tumors. Data are presented as mean ± SD. The mean level of kidney tumors was set to 1.

(E) A schematic drawing of the experimental protocol using chimeric mice with both reprogrammable alleles and the *Lgr5-EGFP* allele. Macroscopic images of the Dox-withdrawn kidney tumor with the *Lgr5-EGFP* allele showing scattered EGFP signals in the kidney tumor. GFP immunostaining of kidney tumor sections revealed that the GFP signals are detectable specifically in tumor cells. Scale bar, 100 μm.

(legend continued on next page)